

## Synthesis of highly active and visible-light-driven PrFeO<sub>3</sub> photocatalyst using solution combustion approach and succinic acid as fuel

Anna S. Seroglazova<sup>1,2,a</sup>, Vadim I. Popkov<sup>2,b</sup>

<sup>1</sup>Saint Petersburg State Institute of Technology, St. Petersburg, Russia

<sup>2</sup>Ioffe Institute, St. Petersburg, Russia

<sup>a</sup>[annaseroglazova@yandex.ru](mailto:annaseroglazova@yandex.ru), <sup>b</sup>[vadim.i.popkov@mail.ioffe.ru](mailto:vadim.i.popkov@mail.ioffe.ru)

Corresponding author: Anna S. Seroglazova, [annaseroglazova@yandex.ru](mailto:annaseroglazova@yandex.ru)

PACS 61.46.+w

**ABSTRACT** In this work, nanocrystalline powder of praseodymium orthoferrite was obtained by the solution combustion synthesis using succinic acid as organic fuel. The obtained sample is characterized by techniques of powder x-ray diffraction, scanning and transmission electron microscopy, and UV-Vis diffuse reflectance spectroscopy. The sample was discovered to have a porous, foamy morphology with an average crystallite size of 36.1 nm and a band gap value of 2.1 eV. The study of Fenton-like photocatalytic activity was carried out on the example of the decomposition of the methyl violet dye in the presence of hydrogen peroxide under visible light. The maximum value of the degradation rate constant is 0.0325 min<sup>-1</sup>. The results were compared to the available data obtained for similar systems.

**KEYWORDS** praseodymium orthoferrite, solution combustion method, succinic acid, nanoparticles, photo-Fenton-like reactions, photocatalysis.

**ACKNOWLEDGEMENTS** This work was carried out in accordance with the Grant of the President of the Russian Federation MK-795.2021.1.3. The Authors acknowledge V. N. Nevedomskiy for the help with TEM investigations.

**FOR CITATION** Seroglazova A.S., Popkov V.I. Synthesis of highly active and visible-light-driven PrFeO<sub>3</sub> photocatalyst using solution combustion approach and succinic acid as fuel. *Nanosystems: Phys. Chem. Math.*, 2022, **13** (6), 649–654.

### 1. Introduction

In recent years, a large number of studies have been directed toward the development and study of new functional materials with a wide range of applications. The most interesting ones among such materials are ferrites with different structures and compositions, in particular ferrites, of rare earth elements (REE).

Rare earth orthoferrites belong to a class of complex oxides with the general chemical formula RFeO<sub>3</sub> (R = rare earth element: Ce, La, Gd, or Pr). The enhanced interest in this class of compounds is due to their unusual distorted perovskite-like structure with a space group of *Pbnm/Pnma* [1–3], which provides them with unique chemical and physical properties: electrical, magnetic, and optical. The combination of the unique properties allows the use of REE orthoferrites in the production of ceramic materials, electronic devices, gas sensors, magnetic materials, MRI contrast agents, and catalytic materials [4–6]. The use of REE orthoferrites as photocatalytic materials in the visible region is identified as the most promising area due to the low value of the band gap (2–3 eV), semiconductor properties, and chemical stability [7, 8].

Among the varieties of orthoferrites of rare earth elements, PrFeO<sub>3</sub> praseodymium orthoferrite is known to have good electromagnetic properties, but it also stands out due to its distinguished photocatalytic properties under visible light [9–11]. However, one of the problems associated with the development of catalytic materials is the production of catalysts with a developed surface and a porous structure. To date, a large number of studies devoted to the preparation of PrFeO<sub>3</sub> nanoparticles using synthesis routes such as sol-gel, co-precipitation, the template method, and the solution combustion method have been published [12–17]. The listed methods of synthesis make it possible to obtain nanostructured materials with tuned particle sizes, morphology, and structure, but most of them are power-consuming and do not always allow one to obtain a structure with a developed porous surface, with the exception of synthesis by solution combustion [18–20]. Distinctive features of the method are its versatility, speed, and the possibility of varying synthesis parameters that allow tuning of the structural, morphological, and functional characteristics of the materials, as well as the possibility of transforming it into large-scale industrial production with the manufacturing of high-purity products. The most important synthesis parameter is the type of organic fuel, which provides the process of self-ignition for the reaction mixture and acts as a chelating agent for metal ions. Glycine and metal nitrates are conventionally chosen as reagents for the combustion

solution synthesis. However, this type of fuel does not allow for the formation of particles with a small average size and a developed porous surface [21–24].

The present study aims to produce pure nanopowders based on  $\text{PrFeO}_3$  by solution combustion synthesis with succinic acid as an organic fuel, followed by a mild heat treatment at  $500^\circ\text{C}$ , and to characterize the synthesized sample by a set of methods of physicochemical analysis. The photo-Fenton-like catalytic activity was then investigated using the model reaction of photodegradation of methyl violet in the presence of  $\text{PrFeO}_3$  as a catalyst and hydrogen peroxide.

## 2. Materials and methods

The starting reagents used for the synthesis of  $\text{PrFeO}_3$  praseodymium orthoferrite were praseodymium nitrate hexahydrate ( $\text{Pr}(\text{NO}_3)_3 \cdot 6\text{H}_2\text{O}$ ), iron nitrate nonahydrate ( $\text{Fe}(\text{NO}_3)_3 \cdot 9\text{H}_2\text{O}$ ), succinic acid ( $\text{C}_4\text{H}_6\text{O}_4$ ), as well as distilled water. All the reagents were chemically pure and used as purchased from Neva-Reactiv (Saint Petersburg, Russia). The reaction solution was prepared by dissolving metal nitrate and succinic acid, taken according to the stoichiometric ratio, in 40 ml of distilled water under constant mixing until all components were completely dissolved. The resulting solution was placed in a glassy carbon dish and heated on an electric stove until complete water removal was achieved, followed by self-ignition of the reaction mixture and the formation of the final solid product, which was ground in a mortar until a homogeneous bright brown powder was formed. The powder was then subjected to heat treatment at  $500^\circ\text{C}$  for 1 hour in an air atmosphere to remove unreacted residues of nitrates and organics.

The elemental composition and morphology of the synthesized  $\text{PrFeO}_3$  particles were studied by scanning electron microscopy using a Tescan Vega 3 SBH microscope equipped with an Oxford INCA 200 electron probe microanalyzer. Analysis of structure and phase composition was performed via powder x-ray diffraction on a Rigaku Smart Lab 3 diffractometer using  $\text{Cu}_{K\alpha 1}$  irradiation ( $\lambda=0.154056$  nm). For a more detailed assessment of the morphology and microstructure, transmission electron microscopy was performed on a JEOL TEM-100CX microscope. Diffuse reflectance spectra were measured with an Avaspec-ULS2048 spectrometer equipped with an AvaSphere-30-Refl integrating sphere.

Methyl violet (MV) was chosen as a model dye for studying photocatalytic activity. The photodegradation process was carried out in an insulated box equipped with a light source with a wavelength of  $\lambda \geq 420$  nm, a magnetic stirrer for constant stirring of the reaction solution, and a 50-ml graduated cylinder.

The experiment included the preparation of a reaction solution containing a dye, a catalyst ( $\text{PrFeO}_3$ ), and hydrogen peroxide ( $\text{H}_2\text{O}_2$ ) with a concentration of 0.0232 g/L, 0.25 g/L, and 0.24 mol/L, respectively. The volume of the solution was 30 mL. Before the start of the experiment, the solution was stirred in the dark for 30 minutes to establish adsorption equilibrium. After that, it was irradiated with a visible light source for 60 minutes with sampling of 5 ml every 10 minutes to determine the MF concentration. Changes in the dye concentration were recorded using an Avaspec-ULS208 spectrometer.

## 3. Results and discussion

Elemental analysis of the combustion products and X-ray diffraction data collected on the initial and heat-treated samples are shown in Fig. 1.

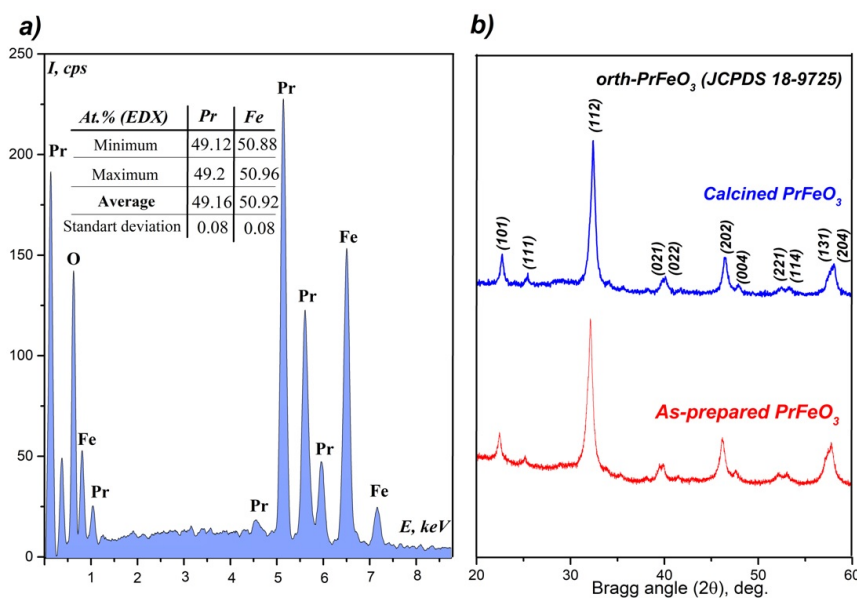


FIG. 1. The energy dispersive X-ray spectroscopy (a) and powder X-ray diffraction patterns (b) of the as-prepared and heat-treated  $\text{PrFeO}_3$  samples

According to the presented results (Fig. 1a), the elemental composition of the synthesis product corresponds to  $\text{PrFeO}_3$ , as evidenced by the presence of three main spectral lines belonging to the key elements: praseodymium (Pr), iron (Fe), and oxygen (O). Within the method's error, the quantitative ratio Pr:Fe in the obtained sample was 49.16 and 50.92 at.%, which is very close to praseodymium orthoferrite in terms of stoichiometry. Detailed results of EDX measurements in terms of Fe and Pr are presented in the table in Fig. 1a.

The X-ray powder diffraction patterns shown in Fig. 1b indicate the formation of only one crystalline phase of praseodymium orthoferrite before and after the heat treatment of the combustion products of the mixture. The crystal structure of the heat-treated product was refined by the Rietveld method. According to the refinement results, the unit cell parameters are in good agreement with the data of JCPDS card No. 18-9725 and are as follows:  $a=5.4858(4)$ ,  $b=5.5756(2)$ ,  $c=7.7898(7)$  Å which corresponds to the space group  $Pbnm$ . The data obtained are also consistent with the results of other studies on the production of  $\text{PrFeO}_3$  by the methods of glycine-nitrate synthesis, microwave, and hydrothermal synthesis [9, 13, 25]. The average crystallite size calculated from the broadening of X-ray diffraction lines for the initial sample was 27.9 nm. After the heat treatment, a slight increase in size up to 36.1 nm is observed, which indicates the process of recrystallization into larger crystals upon moderate heating. It should be noted that  $\text{PrFeO}_3$  synthesized by solution combustion using succinic acid at a stoichiometric ratio has smaller crystallite sizes than  $\text{PrFeO}_3$  synthesized by a similar method, but using glycine as a fuel (57.9 nm) [13].

According to SEM and TEM analysis (Fig. 2b), the morphology of the combustion product after finishing heat treatment is spongy with a developed system of micron and submicron pores, which is typical for many substances, particularly simple and complex oxides obtained by a similar synthesis method [26–28]. The formation of agglomerates consisting of individual  $\text{PrFeO}_3$  particles is also observed, which is associated both with high temperatures in the reaction zone during combustion and with the thermal treatment of the product, which leads to an increase in mass transfer processes. A more detailed study of these processes was previously studied using the examples of the  $\text{YFeO}_3$  [24] and  $\text{NiO}$  [29] systems.

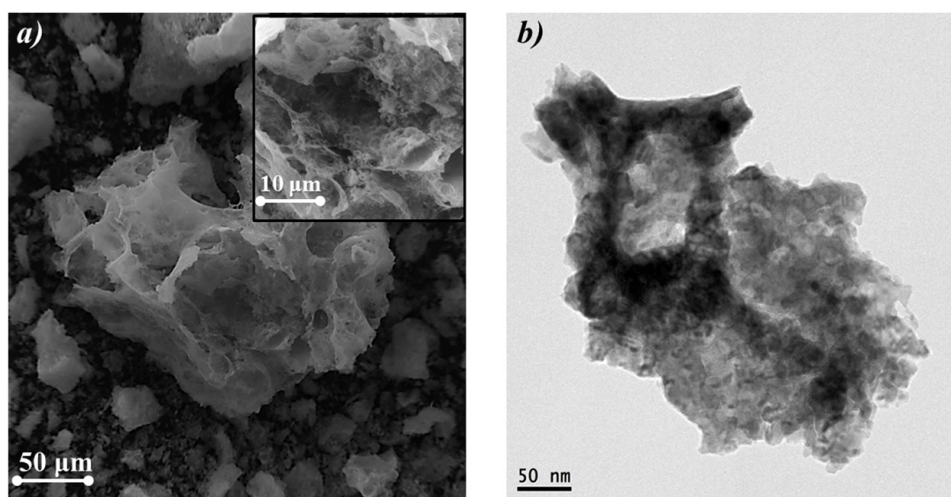


FIG. 2. SEM (a) and TEM (b) images of calcined  $\text{PrFeO}_3$  nanopowder

To describe the optical characteristics of the sample, diffuse reflectance spectroscopy in the UV-Vis region was carried out, the results of which are shown in Fig. 3.

The spectrum shown in Fig. 3a shows a wide absorption band in the wavelength range from 500 nm to 700 nm, corresponding to the visible region of light. The value of the band gap, recalculated in accordance with the Kubelka-Munk transformation and presented in the Tauc coordinates, is shown in Fig. 3b and is 2.1 eV, which is consistent with the literature data [12, 13, 17].

The combination of the research results from powder X-ray diffraction, SEM analysis, and diffuse reflection spectroscopy makes it possible to assume that the synthesized sample can act as a promising photocatalyst in the visible region. It is possible due to its porous structure and small crystallite sizes, which provide greater access for reagents to the catalyst surface area, as well as due to the small value of the band gap, which, when irradiated with visible light, allows for an electron to pass from the valence band to the conduction band with the subsequent formation of a powerful oxidizing hydroxyl radical [13, 30, 31].

The study of the functional properties of  $\text{PrFeO}_3$  in a photocatalytic Fenton-like oxidation process was carried out on the example of the decomposition of the model methyl violet (MV) dye under the action of visible light. The results of the study are shown in Fig. 4.

Fig. 4a shows the typical absorption spectra of methyl violet during photo-Fenton-like degradation. According to the obtained data, in all spectra, there is a single absorption peak corresponding to 550 nm, which naturally decreases

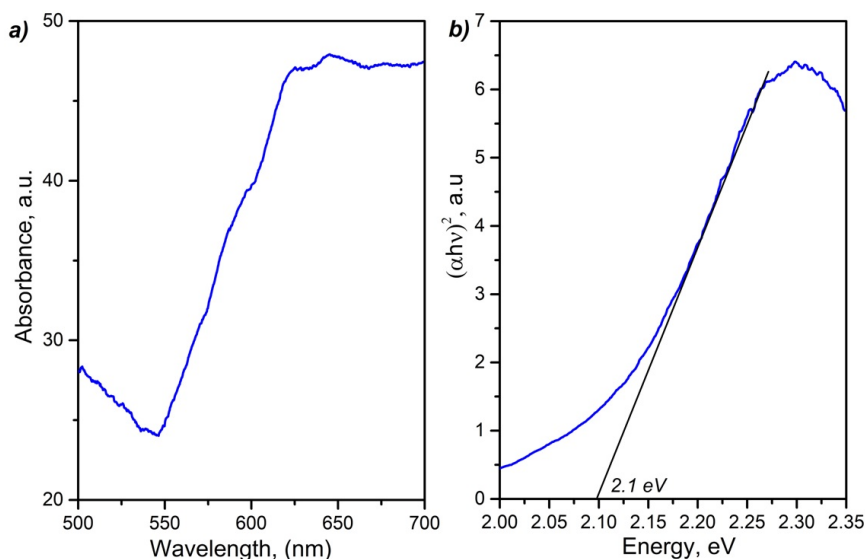


FIG. 3. UV-Vis spectrum of  $\text{PrFeO}_3$  (a) and the corresponding Tauc plot (b)

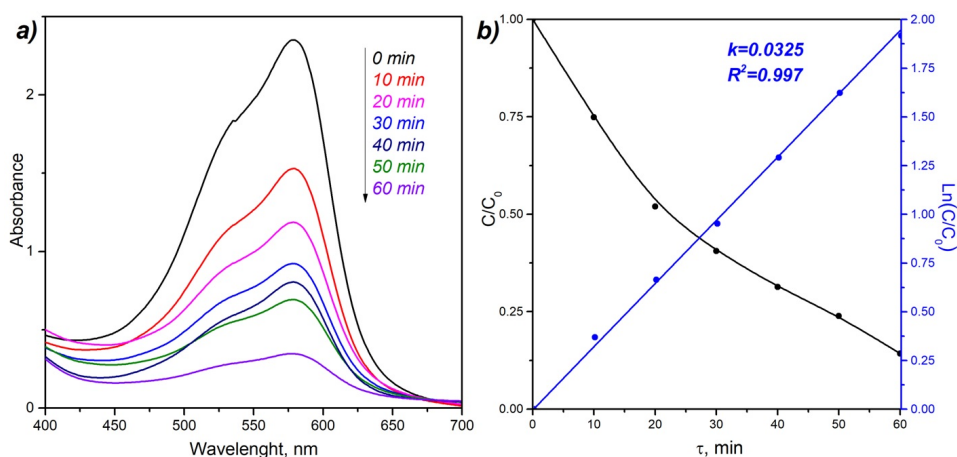


FIG. 4. UV-Vis absorption spectra of methyl violet during photo-Fenton-like degradation (a) and corresponding kinetic curves (b)

with time during prolonged irradiation with a light source, which confirms the photocatalytic activity of the synthesized sample. The most intense decrease in the dye concentration is observed in the first 10 minutes of irradiation, then the intensity of discoloration decreases, which is associated with a gradual decrease in the generation of hydroxyl radicals caused by the processes of recombination of electron-hole pairs [13, 32] and the peculiarity of the filling of catalytically active centers on the catalyst surface.

Based on the experimental data, kinetic studies were also carried out, the results of which are shown in Fig. 4b. As noted earlier, the relative concentration of the dye decreases regularly with the course of irradiation, and in accordance with the shape of the kinetic dependence, it refers to the pseudo-first order of the reaction. The rate constant was calculated by linearizing the kinetic dependence in logarithmic coordinates. The obtained value was  $0.0325 \text{ min}^{-1}$ , which is higher compared to other rare-earth ferrites and orthoferrites (Table 1).

#### 4. Conclusion

Thus, within the framework of this work, the possibility of obtaining pure nanocrystalline praseodymium orthoferrite by combustion in solution using succinic acid as a fuel was shown. According to the results of comparison with the literature data, the obtained particles have a smaller crystallite size (36.1 nm) than in similar synthesis using a standard fuel, glycine (57.9 nm), which makes it possible to vary the particle size, morphology, and specific surface area using different types of fuel. Analysis of photocatalytic activity showed high efficiency in the photo-Fenton-like degradation of methyl violet with a rate constant of  $0.0325 \text{ min}^{-1}$ .

TABLE 1. Comparison of rare earth orthoferrites as visible-light-driven photocatalysts depending on rare earth element, synthesis method and crystallite size

No	Photocatalyst	Synthesis method	Crystallite size, nm	Dye	k, min <sup>-1</sup>	Reference
1	YbFeO <sub>3</sub>	Solution combustion synthesis	54.6	Methyl Violet	0.0040	[33]
2	EuFeO <sub>3</sub>	Sol-gel synthesis	25.2	Rhodamine B	0.0020	[31]
3	NiFe <sub>2</sub> O <sub>4</sub>	Solution combustion synthesis	27.0	Methylene blue	0.0080	[34]
4	PrFeO <sub>3</sub>	Solution combustion synthesis	36.1	Methyl Violet	0.0325	This work

## References

- [1] Lone I.H., Aslam J., Radwan N.R.E., Bashal A.H., Ajlouni A.F.A., Akhter A. Multiferroic ABO<sub>3</sub> Transition Metal Oxides: a Rare Interaction of Ferroelectricity and Magnetism. *Nanoscale Research Letters*, 2019, **14**, P. 1–12.
- [2] Popkov V.I., Tugova E.A., Bachina A.K., Almyasheva O.V. The formation of nanocrystalline orthoferrites of rare-earth elements XFeO<sub>3</sub> (X = Y, La, Gd) via heat treatment of coprecipitated hydroxides. *Russian Journal of General Chemistry*, 2017, **87**, P. 2516–2524.
- [3] Akbashev A.R., Semisalova A.S., Perov N.S., Kaul A.R. Weak ferromagnetism in hexagonal orthoferrites RFeO<sub>3</sub> (R = Lu, Er-Tb). *Applied Physics Letters*, 2011, **99**, P. 2011–2014.
- [4] Xu H, Hu X, Zhang L. Generalized low-temperature synthesis of nanocrystalline rare-earth orthoferrites LnFeO<sub>3</sub> (Ln = La, Pr, Nd, Sm, Eu, Gd). *Crystal Growth and Design*, 2008, **8**, P. 2061.
- [5] Li M., Tan H., Duan W. Hexagonal rare-earth manganites and ferrites: A review of improper ferroelectricity, magnetoelectric coupling, and unusual domain walls. *Physical Chemistry Chemical Physics. Royal Society of Chemistry*, 2020, **22**, P. 14415–14432.
- [6] Mir F.A., Sharma S.K., Kumar R. Magnetizations and magneto-transport properties of Ni-doped PrFeO<sub>3</sub> thin films. *Chinese Physics B*, 2014, **23**.
- [7] Kondrashkova I.S., Martinson K.D., Zakharova N.V., Popkov V.I. Synthesis of Nanocrystalline HoFeO<sub>3</sub> Photocatalyst via Heat Treatment of Products of Glycine-Nitrate Combustion. *Russian Journal of General Chemistry*, 2018, **88**, P. 2465–2471.
- [8] Maity R., Sheikh M.S., Dutta A., Sinha T.P. Visible Light Driven Photocatalytic Activity of Granular Pr Doped LaFeO<sub>3</sub>. *Journal of Electronic Materials*, 2019, **48**, P. 4856–4865.
- [9] Qin C., Li Z., Chen G., Zhao Y., Lin T. Fabrication and visible-light photocatalytic behavior of perovskite praseodymium ferrite porous nanotubes. *Journal of Power Sources*, 2015, **285**, P. 178–184.
- [10] Arakawa T., Tsuchi-Ya S.I., Shiohara J. Catalytic properties and activity of rare-earth orthoferrites in oxidation of methanol. *Journal of Catalysis*, 1982, **74**, P. 317–322.
- [11] Megarajan S.K., Rayalu S., Nishibori M., Labhsetwar N. Improved catalytic activity of PrMO<sub>3</sub> (M = Co and Fe) perovskites: Synthesis of thermally stable nanoparticles by a novel hydrothermal method. *New Journal of Chemistry*, 2015, **39**, P. 2342–2348.
- [12] Wang X., Cao S., Wang Y., Yuan S., Kang B., Wu A., et al. Crystal growth and characterization of the rare earth orthoferrite PrFeO<sub>3</sub>. *Journal of Crystal Growth*, 2013, **362**, P. 216–219.
- [13] Seroglazova A.S., Lebedev L.A., Chebanenko M.I., Sklyarova A.S., Buryanenko I.V., Semenov V.G., et al. Ox/Red-controllable combustion synthesis of foam-like PrFeO<sub>3</sub> nanopowders for effective photo-Fenton degradation of methyl violet. *Advanced Powder Technology*, 2022, **33**, P. 103398.
- [14] Nguyen A.T., Nguyen V.Y., Mittova I.Y., Mittova V.O., Viryutina E.L., Hoang C.C.T., et al. Synthesis and magnetic properties of PrFeO<sub>3</sub> nanopowders by the co-precipitation method using ethanol. *Nanosystems: Physics, Chemistry, Mathematics*, 2020, **11**, P. 468–473.
- [15] Abdellahi M., Abhari A.S., Bahmanpour M. Preparation and characterization of orthoferrite PrFeO<sub>3</sub> nanoceramic. *Ceramics International*, 2016, **42**, P. 4637–4641.
- [16] Freeman E., Kumar S., Thomas S.R., Pickering H., Fermin D.J., Eslava S. PrFeO<sub>3</sub> Photocathodes Prepared Through Spray Pyrolysis. *ChemElectroChem*, 2020, **7**, P. 1365–1372.
- [17] Tang P., Xie X., Chen H., Lv C., Ding Y. Synthesis of Nanoparticulate PrFeO<sub>3</sub> by Sol–Gel Method and its Visible-Light Photocatalytic Activity. *Ferroelectrics*, 2019, **546**, P. 181–187.
- [18] Wen W., Wu J.M. Nanomaterials via solution combustion synthesis: A step nearer to controllability. *RSC Advances*, 2014, **4**, P. 58090–58100.
- [19] Zhu C., Akiyama T. Optimized conditions for glycine-nitrate-based solution combustion synthesis of LiNi<sub>0.5</sub>Mn<sub>1.5</sub>O<sub>4</sub> as a high-voltage cathode material for lithium-ion batteries. *Electrochimica Acta*, 2014, **127**, P. 290–298.
- [20] Mukasyan A.S., Epstein P., Dinka P. Solution combustion synthesis of nanomaterials. *Proceedings of the Combustion Institute*, 2007, **31**, P. 1789–1795.
- [21] Tugova E., Yastrebov S., Karpov O., Smith R. NdFeO<sub>3</sub> nanocrystals under glycine nitrate combustion formation. *Journal of Crystal Growth*, 2017, **467**, P. 88–92.
- [22] Bachina A., Ivanov V.A., Popkov V.I. Peculiarities of LaFeO<sub>3</sub> nanocrystals formation via glycine-nitrate combustion. *Nanosystems: Physics, Chemistry, Mathematics*, 2017, **8**, P. 647–653.
- [23] Komova O.V., Simagina V.I., Mukha S.A., Netskina O.V., Odegova G.V., Bulavchenko O.A., et al. A modified glycine-nitrate combustion method for one-step synthesis of LaFeO<sub>3</sub>. *Advanced Powder Technology*, 2016, **27**, P. 496–503.
- [24] Popkov V.I., Almyasheva O.V., Nevedomskiy V.N., Sokolov V.V., Gusarov V.V. Crystallization behavior and morphological features of YFeO<sub>3</sub> nanocrystallites obtained by glycine-nitrate combustion. *Nanosystems: Physics, Chemistry, Mathematics*, 2015, **6**, P. 866–874.
- [25] Tijare S.N., Bakardjieva S., Subrt J., Joshi M.V., Rayalu S.S., Hishita S., et al. Synthesis and visible light photocatalytic activity of nanocrystalline PrFeO<sub>3</sub> perovskite for hydrogen generation in ethanol-water system. *Journal of Chemical Sciences*, 2014, **126**, P. 517–525.
- [26] Mukasyan A.S., Dinka P. Novel approaches to solution-combustion synthesis of nanomaterials. *International Journal of Self-Propagating High-Temperature Synthesis*, 2007, **16**, P. 23–35.
- [27] Popkov V.I., Martinson K.D., Kondrashkova I.S., Enikeeva M.O., Nevedomskiy V.N., Panchuk V.V., et al. SCS-assisted production of EuFeO<sub>3</sub> core-shell nanoparticles: formation process, structural features and magnetic behavior. *Journal of Alloys and Compounds*, 2021, **859**, P. 157812.
- [28] Petschnig L.L., Fuhrmann G., Schildhammer D., Tribus M., Schottenberger H., Huppertz H. Solution combustion synthesis of CeFeO<sub>3</sub> under ambient atmosphere. *Ceramics International*, 2016, **42**, P. 4262–4267.

- [29] Wolf E.E., Manukyan K.V., Cross A., Roslyakov S., Rouvimov S., Rogachev A.S., et al. Solution Combustion Synthesis of Nano-Crystalline Metallic Materials: Mechanistic Studies. *The Journal of Physical Chemistry C*, 2013, **117**, P. 24217–24227.
- [30] Sarikhani F., Zabardasti A., Reza A., Mahmoud S. Enhanced visible light activity of – EuFeO<sub>3</sub>/TiO<sub>2</sub> nanocomposites prepared by thermal treatment – hydrolysis precipitation method. *Applied Physics*, 2020, **126**, P. 476.
- [31] Ju L., Chen Z., Fang L., Dong W., Zheng F., Shen M. Sol-gel synthesis and photo-Fenton-like catalytic activity of EuFeO<sub>3</sub> nanoparticles. *Journal of the American Ceramic Society*, 2011, **94**, P. 3418–3424.
- [32] Tikhanova S.M., Lebedev L.A., Kirillova S.A., Tomkovich M.V., Popkov V.I. Synthesis, structure, and visible-light-driven activity of o-YbFeO<sub>3</sub>/h-YbFeO<sub>3</sub>/CeO<sub>2</sub> photocatalysts. *Chimica Techno Acta*, 2021, **8**, P. 20218407.
- [33] Tikhanova S.M., Lebedev L.A., Martinson K.D., Chebanenko M.I., Burianenko I.V., Semenov V.G., Nevedomskiy V.N., Popkov V.I. Synthesis of novel heterojunction h-YbFeO<sub>3</sub>/o-YbFeO<sub>3</sub> photocatalyst with enhanced Fenton-like activity under visible-light. *New Journal Chemistry*, 2020, **45**, P. 1541–1550.
- [34] Martinson K.D., Belyak V.E., Sakhno D.D., Kiryanov N.V., Chebanenko M.I., Popkov V.I. Effect of fuel type on solution combustion synthesis and photocatalytic activity of NiFe<sub>2</sub>O<sub>4</sub> nanopowders. *Nanosystems: Physics, Chemistry, Mathematics*, 2021, **12**, P. 792–798.

---

*Submitted 28 August 2022; accepted 1 December 2022*

*Information about the authors:*

*Anna S. Seroglazova* – Saint Petersburg State Institute of Technology, 26 Moskovsky prospect, St. Petersburg, 190013 Russia; Ioffe Institute, St. Petersburg, 194021 Russia; ORCID 0000-0002-3304-9068; annaseroglazova@yandex.ru

*Vadim I. Popkov* – Ioffe Institute, St. Petersburg, 194021 Russia; ORCID 0000-0002-8450-4278; vadim.i.popkov@mail.ioffe.ru

*Conflict of interest:* the authors declare no conflict of interest.